metals

MDPI

Article

Evolution of the Microstructure and Mechanical Properties of a Ti35Nb2Sn Alloy Post-Processed by Hot Isostatic Pressing for Biomedical Applications

Joan Lario *, Ángel Vicente and Vicente Amigó

Universitat Politècnica de València, DIMM ETSII, Camino de Vera s/n, 5E Building, 46022 Valencia, Spain; avicente@mcm.upv.es (Á.V.); vamigo@mcm.upv.es (V.A.)
* Correspondence: joalafe@upv.es

Abstract: The HIP post-processing step is required for developing next generation of advanced powder metallurgy titanium alloys for orthopedic and dental applications. The influence of the hot isostatic pressing (HIP) post-processing step on structural and phase changes, porosity healing, and mechanical strength in a powder metallurgy Ti35Nb2Sn alloy was studied. Powders were pressed at room temperature at 750 MPa, and then sintered at 1350 °C in a vacuum for 3 h. The standard HIP process at 1200 °C and 150 MPa for 3 h was performed to study its effect on a Ti35Nb2Sn powder metallurgy alloy. The influence of the HIP process and cold rate on the density, microstructure, quantity of interstitial elements, mechanical strength, and Young's modulus was investigated. HIP post-processing for 2 h at 1200 °C and 150 MPa led to greater porosity reduction and a marked retention of the β phase at room temperature. The slow cooling rate during the HIP process affected phase stability, with a large amount of α''-phase precipitate, which decreased the titanium alloy's yield strength.

Keywords: hot isostatic pressing; β-Type titanium alloy; biomaterial; phase transformation; powder metallurgy

Citation: Lario, J.; Vicente, Á.; Amigó, V. Evolution of the Microstructure and Mechanical Properties of a Ti35Nb2Sn Alloy Post-Processed by Hot Isostatic Pressing for Biomedical Applications. *Metals* **2021**, *11*, 1027. https://doi.org/10.3390/met11071027

Academic Editor: Maciej Motyka

Received: 8 June 2021
Accepted: 23 June 2021
Published: 25 June 2021

1. Introduction

The low elastic modulus of titanium alloys has replaced other metallic alloys, such as Co-Cr alloys and stainless steels (316L or 307), for load-bearing orthopaedic and dental implants [1,2]. The bone reabsorption issue is related to the stress shielding effect, which occurs due to a stiffness mismatch between implant and bone. Beta titanium alloys present the lowest Young's modulus by both enhancing the stress transmission between the bone and the implant and inhibiting bone resorption [2–4].

The development of low-modulus high-strength beta titanium alloys is essential for the next generation of material prostheses to prolong implant lifetime beyond 15 years, which has been the standard for the past 50 years for Ti Cp and Ti6Al4V ELI alloys [5]. Mechanical properties are directly connected to their metallurgical processing routes, chemical composition, and stabilised phases. The refractory elements added to stabilise the titanium beta phase (Nb, Mo, Ta, Zr) have a high melting point and a large difference in specific gravity, which seriously complicate the melting process, which requires 6–10 remelting steps followed by a homogenising annealing treatment to increase chemical and phase homogeneity [6,7]. The vacuum melting technologies (VIM, VAR, EBM) employed to obtain titanium alloys are complex and expensive, use considerable energy, and often involve supplier delivery lead times of around 35 weeks [8–10].

Powder metallurgy (PM) technology is an alternative processing route to obtain beta titanium alloys, where the alloying elements used to stabilise the β phase can be incorporated into the solid state during sintering. Conventional PM titanium alloys present a

remaining porosity after sintering (2–8 vol%) that can significantly reduce long-time performance. Therefore, the next advanced titanium alloys for the biomedical sector will rely on HIP post-processing to remove residual porosity, which will allow powder metallurgy to be processed by plastic deformation techniques [9–17]. HIP has been used for several decades in the aerospace and automotive industries to improve fatigue, ductility, and fracture toughness [18]. Therefore, it is very important to predict materials' long-term behaviour to design and manufacture reliable implants. To avoid mechanical stress, corrosion, and fatigue problems, titanium alloys must not present porosity, and must have excellent chemical homogeneity. Rapid cooling HIP furnaces enable the HIP cycle to be combined with conventional heat treatment where high cooling rates are required to stabilise the beta phase at room temperature. During a conventional HIP process, titanium powders need to be encapsulated in containers, degassed, and sealed before the hot isostatic press cycle starts. However, in the present study, the beta powder titanium samples were presintered under such conditions with residual porosity below 6% to allow the alloys to be hot isostatic-pressed directly without using containers.

The present paper proposes a processing route to obtain Ti35Nb2Sn based on conventional powder metallurgy (compact and vacuum sintering) and HIP post-processing. It aims to evaluate the effect of the HIP route on beta titanium powder metallurgy alloys (Ti35Nb2Sn) at different cooling rates.

2. Materials and Methods

2.1. Processing Conditions

A new beta titanium alloy with a nominal Ti35Nb2Sn composition was fabricated by using a conventional powder metallurgical route (press and vacuum sintering). Hydride–dehydride titanium powder (99.7%wt purity), niobium powder (99.6%wt), and tin powder (99.6%wt), with a maximum particle size particle of 45 μm, were chosen as the raw materials. Powders were weighed and prepared in an argon chamber GP Campus (Jacomax, Dagneux, France) to avoid oxidation. The mixture was prepared in a shaker mixer Turbula T2F (Willy A Bachofen AG, Muttenz, Switzerland) for 2 h to increase homogeneity. Subsequently, rectangular samples (30 mm× 10 mm× 10 mm) were produced in a double-effect floating die press at 700 MPa pressure. Green compacts were sintered in an HVT 15/75/450 tube vacuum sintering furnace (Carbolite Gero Ltd., Parson, UK) in a high vacuum at $<10^{-4}$ mbars. Samples were heated to 800 °C at 15 °C/min, held at that temperature for 30 min, heated to 1350 °C at 10 °C/min, and finally held for 180 min and cooled at 10 °C/min.

Without using containers, some sintered samples were hot isostatic-pressed under two different conditions. HIP was performed by a Quintus model QIH21 (Quintus Technologies AB, Västerås, Sweden) under the following operation conditions: temperature of 1200 °C, argon gas pressure of 150 MPa, holding time of 2 h and two different cooling rates: 500 °C/min and 100 °C/min (Figure 1). Three scenarios (sintered, HIP1, HIP2) were designed to study the influence of the HIP process on the Ti35Nb2Sn alloys. The conditions for each experiment are found in Table 1.

Table 1. Parameters selected according to Ti35Nb2Sn processing step.

Processing Route	Pressure (MPa)	Maximum Temperature (°C)	Time (minutes)	Cooling Rate (°C/min)
Vacuum Sintering	N/A	1350	180	15
HIP 1 (Fast cooling)	150	1200	120	500
HIP 2 (Slow cooling)	150	1200	120	100

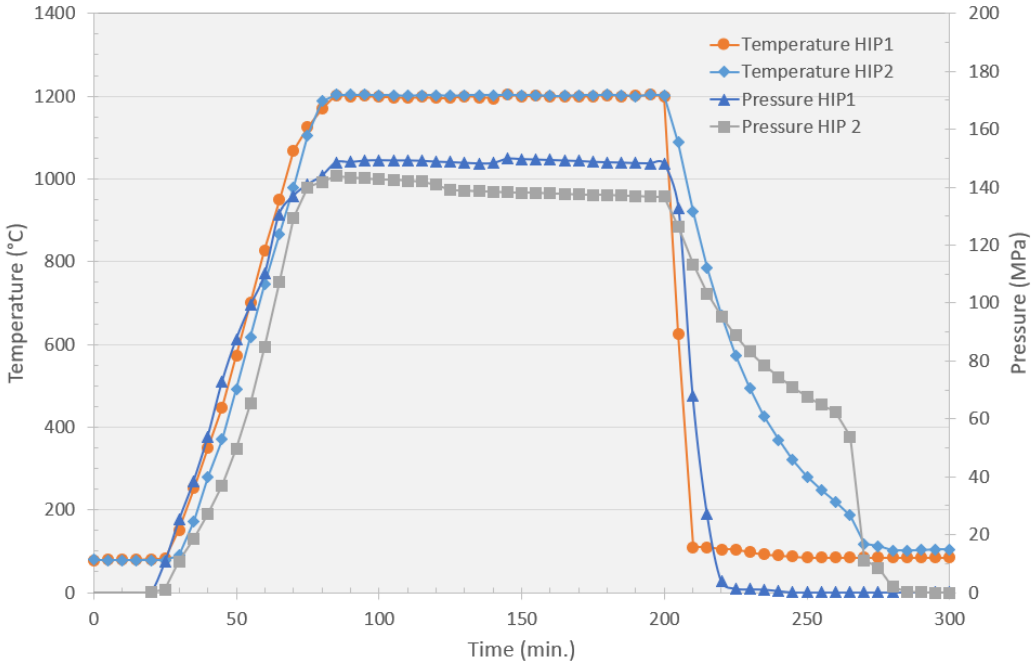

Figure 1. Temperature and pressure evolution during Hot Isostatic Pressing performed on Quintus QIH21 equipment.

2.2. Characterization

The relative density for each scenario was measured based on Archimedes' principle in accordance with ASTM standard C373-88. Tensile specimens were tested by a Shimadzu AG-X plus mechanical tester (Shimadzu, Kyoto, Japan) at a crosshead speed of 0.5 mm/min on three points bending test per standard ISO 3325. The ultrasonic technique was selected to measure Young's modulus, for which the Sonelastic CA-DP equipment was employed (ATCP Ingeniería Física, Ribeirao Preto, Brazil). At least five test specimens with size of 30 mm× 10 mm× 10 mm were measured from each processing condition.

The optical microscopy study (LV100 Nikon, Tokyo, Japan) was performed on the polished samples to observe internal residual porosity. To observe phases present in Ti35Nb2Sn according to the processing route, the mechanically polished samples were etched in Kroll's reagent to reveal their microstructure and to be viewed by optical microscopy. Grain size and orientation, morphology, and phase distribution surface were characterised by a Scanning Electron Microscope (SEM, ZEISS, Oberkochen, Germany) and an Electron Backscatter Diffraction (EBSD) detector. The EBSD operated at 20 kV and 5 nA, and step size was set at 0.05 µm on a sample tilted 70° from the horizontal for orientation mapping. The elemental analyses of the different processing routes were carried out by Energy Dispersive Spectroscopy (EDS) from Oxford Instruments Ltd. (Abingdon-on-Thames, UK).

3. Results and Discussion

The alloy's microstructure is one of the main factors controlling its tensile strength, wear resistance, and corrosion resistance. Table 2 shows the variation in density, phases, and average grains of the Ti35Nb2Sn alloy under different manufacturing conditions. The samples presented high densification, around 75% of the theoretical density after pressing, and approximately 98% after the sintering cycle, which was higher than 99% after HIP post-processing. As the percentage of the retained β phase was above 20% at room temperature, the three processing conditions for Ti35Nb2Sn allowed classification in the β titanium alloys category.

Table 2. Archimedes' and metallographic characterization of the Ti35Nb2Sn alloy.

Processing Route	Green Density (%)	Relative Density (%)	β Phase (%)	α + β Phase (%)	Grain Size (μm)
Vacuum Sintering	80.2 ± 0.5	94.9 ± 0.1	38.4	56.5	19.1 ± 11.3
HIP 1 (Fast cooling)		100.1 ± 0.2	95.5	3.7	57.2 ± 32.3
HIP 2 (Slow cooling)		100.2 ± 0.1	78.9	20.8	55.2 ± 33.5

The microstructures of the tested alloys are presented in Figure 2. The α-phase areas decreased with a rising HIP cooling rate. A heterogeneous phase composition was observed on the sintered and HIP 2 samples, composed predominantly by a β equiaxial grain, with small areas with the α+β phase (Figure 2A,C). As both temperature and pressure increased due to the HIP cycle, plastic deformation on the sintered samples took place. The HIP temperature above the beta transus temperature was required to reduce yield stress, and to enhance creep under pressure, to improve diffusion efficiency and remove residual porosity in a reasonable time (Table 2). The obtained data show that HIP post-processing gave relievable and repeatable results. The HIP process also significantly influenced the enlarged grain size. Initially for the sintered sample, the average grain size was around 19 μm and then increased to 55 μm after HIP post-processing increased (Table 2).

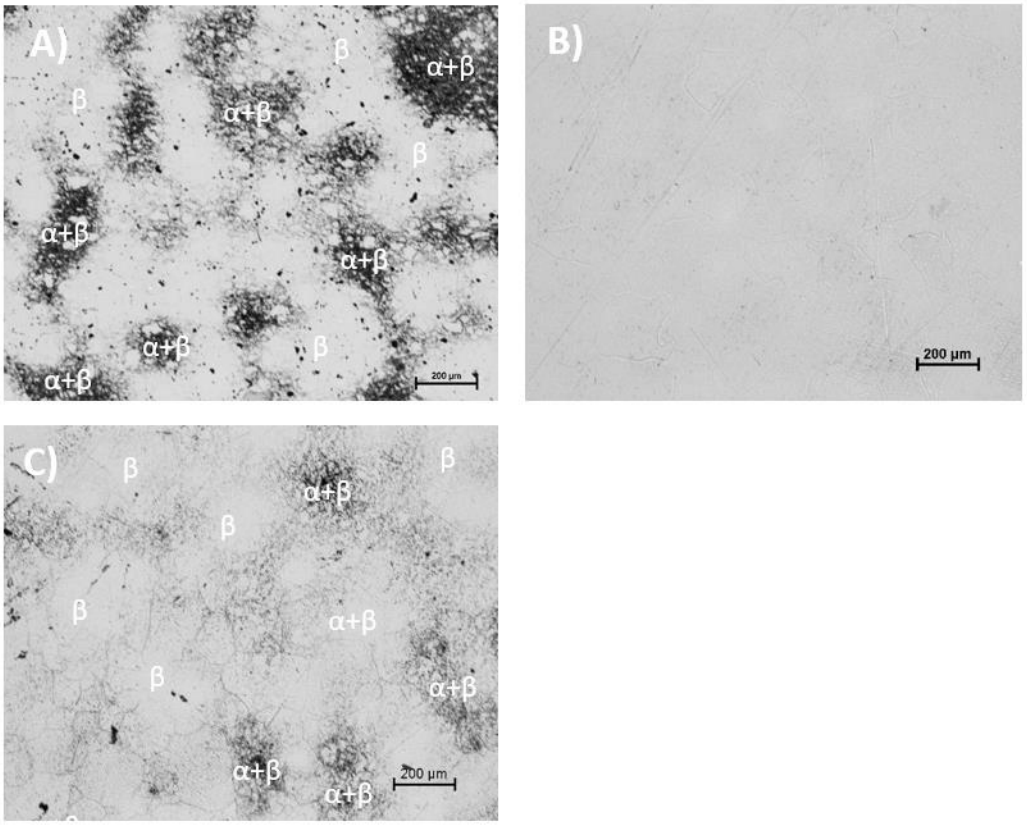

Figure 2. The microstructure of Ti35Nb2Sn according to its manufacturing condition. (**A**) Conventional vacuum sintering at 1350 °C for 180 min. (**B**) HIPed under 1200 °C, 150 MPa, and cooling rate 500 °C/min. (HIP 1) (**C**) HIPed under 1200 °C, 150 MPa, and cooling rate 100 °C/min (HIP 2).

Nowadays, thermo-mechanical deformation metallurgical processes (forge, cold rolling, hot drawing) are employed to modify grain size, ductility, and materials' tenacity [19,20]. This type of process cannot be performed on powder metallurgical material if residual porosity is higher than 2% because of the work hardening that materials present, which tends to fracture in the confirmation process. The present study corroborates that

the inclusion of the HIP cycle after sintering on the beta titanium manufacturing route drastically reduced residual porosity, which allowed powder metallurgical titanium alloys to be submitted to the plastic deformation metallurgical process to obtain advanced titanium alloys. The mechanical–corrosion properties of titanium alloys depend on not only chemical and phase homogeneity, but also on morphology and grain size. This study shows that metastable β-type Ti35Nb2Sn alloys can be obtained when a 500°C/min cooling rate is employed during HIP post-processing (Figure 2B).

Figure 3 shows the Ti35Nb2Sn microstructures after performing HIP processing under different conditions from various scales by SEM and EBSD. The EBSD images demonstrated that the previous α+β areas detected by optical microscopy were actually α″ precipitates at the β matrix (Figure 3B). The phases present at the microscopic level became more homogeneous, with no pronounced differences between the red (β phase) and yellow (α″ phase) areas after sintering and HIP processing. The EBSD analysis corroborated that the second HIP scenario, in which the titanium alloy was cooled more slowly from the β field to room temperature at 100°C/min instead of at 500°C/min, presented more intragranular α″ precipitates around 32%, compared with 5% quantified on the rapid cooling samples (HIP 1). During rapid cooling from the β-phase stability temperature range, diffusion can be restricted, and stable α phase formation prevented. Since the current Ti35Nb2Sn presents an elevated amount of beta alloying elements, α-martensite's hexagonal structure becomes distorted, and the crystalline structure loses its hexagonal symmetry to acquire an orthorhombic structure (α″-martensite).

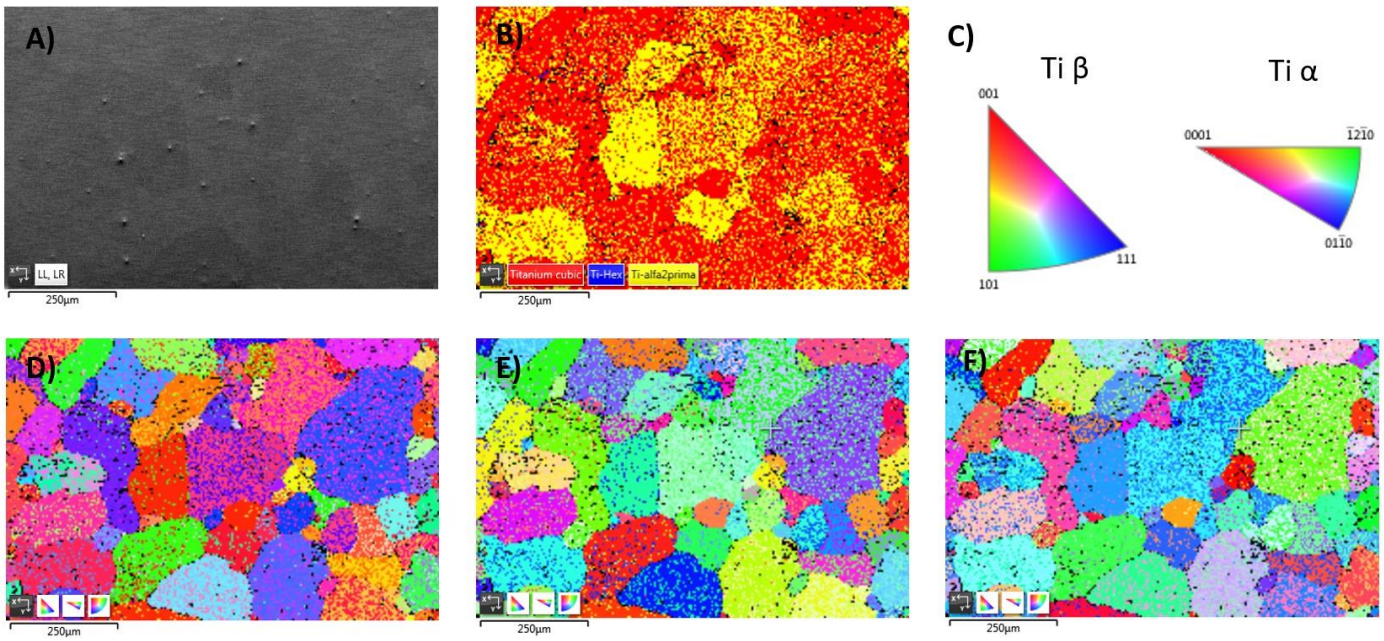

Figure 3. The microstructure of Ti35Nb2Sn after HIPping under 1200 °C, 150 MPa, and cooling rate 100 °C/min (HIP 2). (**A**) SEM image. (**B**) images showing the α″ precipitates. (**C**) crystallographic orientation for β and α phase. (**D**–**F**) Inverse pole figures (IPF) for X, Y, and Z reference direction maps highlighting grains.

The SEM images and corresponding EDS mappings presented more significant information about alloying element distribution and diffusion on the titanium matrix. The microstructural analysis performed in EDS revealed that some parts were not completely homogeneous (Figure 4C). These brighter areas presented low diffusion between niobium and the titanium matrix. The HIP cycle allowed the brighter areas to reduce due to the thermo-mechanical treatment, even though the titanium alloy's chemical homogeneity still had room for improvement.

The α+β regions with fewer refractory elements displayed high chemical heterogeneity. The mechanical characteristics obtained on the Ti35Nb2Sn alloy are summarized in

Table 3. The heterogeneity of the titanium phases (β, α, and α''), together with residual porosity, were the main causes for the differences found in the titanium alloy's mechanical properties. Residual porosity reduction increased the percentage of ductility, and also improved Ti35Nb2Sn's mechanical response. The microstructure had a stronger influence on ultimate tensile strength rather than porosity, as reflected by UTS, which lowered from 900 MPa to 700 MPa when the α'' content grew due to the 100 °C/min cooling rate employed in HIP 2, even though porosity decreased in relation to the sintered sample (see Table 3).

Table 3. Mechanical results of the Ti35Nb2Sn alloy.

Processing Route	UTS (MPa)	ε (%)	E (GPa)	G (GPa)	Poisson's Ratio
Vacuum Sintering	993 ± 82	3.44 ± 0.36	70.49 ± 1.09	25.62 ± 0.39	0.38 ± 0.04
HIP 1 (Fast cooling)	997 ± 63	3.31 ± 0.23	71.23 ± 2.04	24.62 ± 0.85	0.45 ± 0.06
HIP 2 (Slow cooling)	702 ± 80	2.65 ± 0.12	72.29 ± 1.04	23.77 ± 1.73	0.53 ± 0.13

Young´s modulus is one of the most crucial mechanical properties to control the load transfer between the implant and bone [1–3]. Given its low elastic modulus, excellent mechanical properties, and greater corrosion resistance, TixNbySn is a promising candidate for medical use [4]. The large amount of beta stabilisers (niobium) in the alloy's composition contributed to lower Young´s modulus, with values of 70 GPa, which improved the current 100 or 110 GPa that today's titanium alloys employed in prosthesis present (Ti CP and Ti6Al4V ELI), and may minimise bone atrophy due to the stress shielding effect, which increases implant durability.

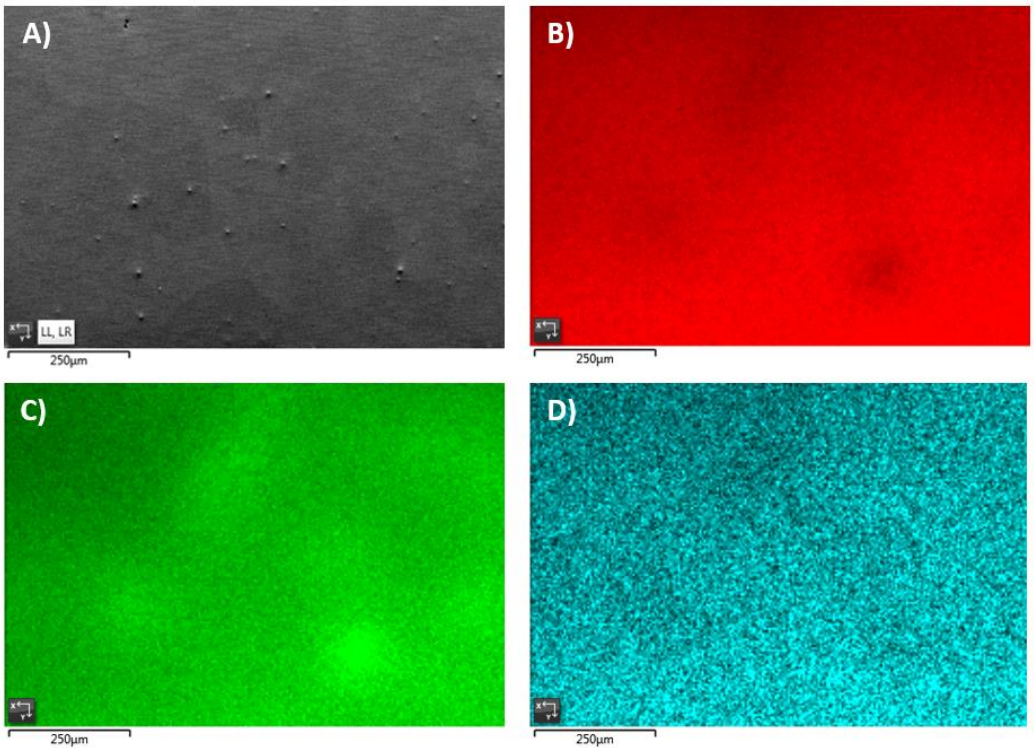

Figure 4. SEM and EDS mapping of Ti, Nb, and Sn respectively, for Ti35Nb2Sn HIPed at 1200 °C, 150 MPa and cooled at 100 °C/min (HIP 2). (**A**) SEM image. (**B**) Titanium EDS mapping. (**C**) Niobium EDS mapping. (**D**) Tin EDS mapping.

L. Tan et al. (2018) studied the precipitation phenomenon, the prior particle boundary (PPB), that occurs during HIPing and justify the lower deformation values on titanium samples. Plastic deformation metallurgic process, such as hot forging, cold drawing, and ECAP, modifies the grain dimension and morphology, minimizing the impact from PPB

precipitation on PM parts, and increasing the strength of the titanium alloys [18]. Li et al. (2011) found that Ti2448 alloys fabricated by powder metallurgy exhibited very limited ductility (~2%) during tensile tests. Their mechanical properties can be substantially improved simply by solution treatment at a suitable temperature, followed by water quenching. After heat treatment, Ti2448 elongation increased to 15% and its Young's modulus lowered to 58.3 MPa [20–22]. Severe plastic deformation fabrication methods draw a great of attention to the β-type biomedical alloys field as they add grain refinement, which significantly increases both strength and fatigue life expectancy [23–25].

Developing an appropriate microstructure with optimum mechanical properties and good corrosion resistance is a challenging problem in the low modulus β-type titanium alloys field, which should be addressed in the biomedical industrial sector. This would imply the inclusion of an advanced thermo-mechanical process, such as hot drawing and working or ECAP, heat, and electrochemical treatments [26–29].

4. Conclusions

This study confirms that field-assisted consolidation processes, such as HIP, can be employed to reduce residual porosity and to increase the chemical and phase homogeneity of beta powder metallurgy titanium alloys required for further developing advanced titanium alloys for the biomedical field. When applying HIP at 1200°C and 150 MPa for 3 h to pre-sintered Ti35Nb2Sn samples, a high degree of densification occurs, which allows residual porosity to close and the density theoretical value to be obtained. As the cooling rate during the HIP process lowers from 500 °C/min (HIP 1) to 100°C/min (HIP 2), the phase transformation from the β phase (bcc) to the α phase (hcp) is restricted and the supersaturated α'' phase appears, which diminishes Ti35Nb2Sn yield strength and elongation.

Author Contributions: J.L. and V.A. carried out the experiment. J.L. wrote the manuscript with support from V.A. The samples were fabricated by J.L. and Á.V.; Á.V. and V.A. helped supervise the project. All authors provided critical feedback and helped shape the research, analysis, and manuscript. All authors have read and agreed to the published version of the manuscript.

Funding: This research was funded by Spanish Ministry of Economy and Competitiveness, Research Project 553 Project RTI2018-097810-B-I00, and the European Commission via FEDER funds to purchase equipment for research purposes and the Microscopy Service at the Valencia Polytechnic University.

Institutional Review Board Statement: Not applicable.

Informed Consent Statement: Not applicable.

Data Availability Statement: Data available in a publicly accessible repository. The data presented in this study are openly available in FigShare repository at 10.6084/m9.figshare.14444570.

Acknowledgments: Thanks to Johannes Gårdstam and Mat Sjöstedt from Quintus Technologies AB, Sweden for the technical assistance and the realization of the HIP process.

Conflicts of Interest: The authors declare no conflict of interest. The funders had no role in the design of the study; in the collection, analyses, or interpretation of data; in the writing of the manuscript, or in the decision to publish the results.

References

1. Kuroda, D.; Niinomi, M.; Morinaga, M.; Kato, Y.; Yashiro, T. Design and mechanical properties of new β type titanium alloys for implant materials. *Mater. Sci. Eng. A* **1998**, *243*, 244–249, doi:10.1016/s0921-5093(97)00808-3.
2. Long, M.; Rack, H.J. Titanium alloys in total joint replacement—A materials science perspective. *Biomaterials* **1998**, *19*, 1621–1639.
3. Niinomi, M. Mechanical biocompatibilities of titanium alloys for biomedical applications. *J. Mech. Behav. Biomed. Mater.* **2008**, *1*, 30–42, doi:10.1016/j.jmbbm.2007.07.001.
4. Miura, K.; Yamada, N.; Hanada, S.; Jung, T.K.; Itoi, E. The bone tissue compatibility of a new Ti-Nb-Sn alloy with a low Young's modulus. *Acta Biomater.* **2011**, *7*, 2320–2326, doi:10.1016/j.actbio.2011.02.008.

5. Bjursten, L.M.; Rasmusson, L.; Oh, S.; Smith, G.C.; Brammer, K.S.; Jin, S. Titanium dioxide nanotubes enhance bone bonding in vivo. *J. Biomed. Mater. Res. Part A* **2010**, *92*, 1218–1224, doi:10.1002/jbm.a.32463.
6. de Mello, M.G.; Dainese, B.P.; Caram, R.; Cremasco, A. Influence of heating rate and aging temperature on omega and alpha phase precipitation in Ti–35Nb alloy. *Mater. Charact.* **2018**, *145*, 268–276, doi:10.1016/j.matchar.2018.08.035.
7. Málek, J.; Hnilica, F.; Veselý, J.; Smola, B. Heat treatment and mechanical properties of powder metallurgy processed Ti-35.5Nb-5.7Ta beta-titanium alloy. *Mater. Charact.* **2013**, *84*, 225–231, doi:10.1016/j.matchar.2013.08.006.
8. Cui, C.; Hu, B.M.; Zhao, L.; Liu, S. Titanium alloy production technology, market prospects and industry development. *Mater. Des.* **2011**, *32*, 1684–1691, doi:10.1016/j.matdes.2010.09.011.
9. Leyens, C.; Peters, M. *Titanium and Titanium Alloys. Fundamentals and Applications*; WILEY-VCH Verlag GmbH & Co. KGaA: Weinheim, Germany, 2003. ISBN: 3-527-30534-3.
10. Li, Y.; Yang, C.; Zhao, H.; Qu, S.; Li, X.; Li, Y. New Developments of Ti-Based Alloys for Biomedical Applications. Mater. **2014**, 7, 1709–1800, doi:10.3390/ma7031709.
11. Duan, W.; Yin, Y.; Zhou, J.; Wang, M.; Nan, H.; Zhang, P. Dynamic research on Ti6Al4V powder HIP densification process based on intermittent experiments. *J. Alloy. Compd.* **2019**, *771*, 489–497, doi:10.1016/j.jallcom.2018.08.261.
12. Cao, L.; Wu, X.; Zhu, S.; Mei, J.; Wu, X.; Bettles, C. The effect of HIPping pressure on phase transformations in Ti-5Al-5Mo-5V-3Cr. *Mater. Sci. Eng. A* **2014**, *598*, 207–216, doi:10.1016/j.msea.2014.01.013.
13. Dekhtyar, A.I.; Bondarchuk, V.I.; Nevdacha, V.V.; Kotko, A.V. The effect of microstructure on porosity healing mechanism of powder near-β titanium alloys under hot isostatic pressing in α + β-region: Ti-10V-2Fe-3Al. *Mater. Charact.* **2020**, *165*, 110393, doi:10.1016/j.matchar.2020.110393.
14. Atkinson, H.V.; Davies, S. Fundamental aspects of hot isostatic pressing: An overview. *Metall. Mater. Sci.* **2000**, *31*, 2981–3000, doi:10.1007/s11661-000-0078-2.
15. Bolzoni, L.; Ruiz-Navas, E.M.; Zhang, D.; Gordo, E. Modification of sintered titanium alloys by hot isostatic pressing. *Key Eng. Mater.* **2012**, *520*, 63–69, doi:10.4028/www.scientific.net/KEM.520.63.
16. Molaei, R.; Fatemi, A.; Phan, N. Significance of hot isostatic pressing (HIP) on multiaxial deformation and fatigue behaviors of additive manufactured Ti-6Al-4V including build orientation and surface roughness effects. *Int. J. Fatigue* **2018**, *117*, 352–370, doi:10.1016/j.ijfatigue.2018.07.035.
17. Lopez, M.; Pickett, C.; Arrieta, E.; Murr, L.E.; Wicker, R.B.; Ahlfors, M.; Godfrey, D.; Medina, F. Effects of postprocess hot isostatic pressing treatments on the mechanical performance of EBM fabricated TI-6Al-2Sn-4Zr-2Mo. *Materials* **2020**, *13*, 2604, doi:10.3390/ma13112604.
18. Samarov, V.; Seliverstov, D.; Froes, F.H. Fabrication of near-net-shape cost-effective titanium components by use of prealloyed powders and hot isostatic pressing. In *Titanium Powder Metallurgy: Science, Technology and Applications*; Elsevier Inc.: Amsterdam, The Netherlands, 2015, doi:10.1016/B978-0-12-800054-0.00018-6.
19. Yudin, S.N.; Kasimtsev, A.V.; Tabachkova, N.Y.; Sviridova, T.A.; Markova, G.V.; Volod'Ko, S.S.; Alimov, I.A.; Alpatov, A.V.; Titov, D.D. Features of β-Phase Decay in Ti–22Nb–6Zr Alloy. Inorg. Mater. Appl. Res. **2019**, *10*, 1115–1122, doi:10.1134/s2075113319050368.
20. Zherebtsov, S.V.; Dyakonov, G.S.; Salem, A.A.; Malysheva, S.P.; Salishchev, G.A.; Semiatin, S.L. Evolution of grain and subgrain structure during cold rolling of commercial-purity titanium. *Mater. Sci. Eng. A* **2011**, *528*, 3474–3479, doi:10.1016/j.msea.2011.01.039.
21. Tan, L.; He, G.; Liu, F.; Li, Y.; Jiang, L. Effects of temperature and pressure of hot isostatic pressing on the grain structure of powder metallurgy superalloy. *Materials* **2018**, *11*, 328, doi:10.3390/ma11020328.
22. Li, X.; Zhou, Y.; Ebel, T.; Liu, L.; Shen, X.; Yu, P. The influence of heat treatment processing on microstructure and mechanical properties of Ti–24Nb–4Zr–8Sn alloy by powder metallurgy. *Materialia* **2020**, *13*, 100803, doi:10.1016/j.mtla.2020.100803.
23. Li, Z.; Zheng, B.; Wang, Y.; Topping, T.; Zhou, Y.; Valiev, R.Z.; Shan, A.; Lavernia, E.J. Ultrafine-grained Ti-Nb-Ta-Zr alloy produced by ECAP at room temperature. *J. Mater. Sci.* **2014**, *49*, 6656–6666, doi:10.1007/s10853-014-8337-6.
24. Valiev, R.Z.; Semenova, I.P.; Latysh, V.V.; Rack, H.; Lowe, T.C.; Petruzelka, J.; Dluhos, L.; Hrusak, D.; Sochova, J. Nanostructured titanium for biomedical applications. *Adv. Eng. Mater.* **2008**, *10*, 8–11, doi:10.1002/adem.200800026.
25. Langdon, T.G. Processing of ultrafine-grained materials using severe plastic deformation: Potential for achieving exceptional properties. *Rev. Metal. (Madr.)* **2008**, *44*, 556–564, doi:10.3989/revmetalm.0838.
26. Amigó-Borrás, V.; Lario-Femenía, J.; Amigó-Mata, A.; Vicente-Escuder, Á. Titanium, Titanium Alloys and Composites. *Reference Modul. Mater. Sci. Mater. Eng.* **2020**, *1*, doi:10.1016/b978-0-12-819726-4.00044-2.
27. Ahlfors, M.; Hjärne, J.; Shipley, J. Cost effective Hot Isostatic Pressing. A cost calculation study for AM parts. *Quintus Technol.* **2018**, Vol. 12 No. 2, 1–6.
28. Torralba, J.M.; Campos, M. Toward high performance in Powder Metallurgy. *Rev. Metal.* **2014**, *50*, doi:10.3989/revmetalm.017.
29. Lario-Femenía, J.; Amigó-mata, A.; Vicente-escuder, Á.; Segovia-lópez, F. Desarrollo de las aleaciones de titanio y tratamientos superficiales para incrementar la vida útil de los implantes. *Rev. Metal.* **2016**, *52*, 1–13, doi:10.3989/revmetalm.084.